

## Regional Measurement of Respiratory Gas Arrival Time with Hyperpolarized Gas MRI

Kiarash Emami<sup>1</sup>, Yi Xin<sup>1</sup>, Puttisarn Mongkolwisetwara<sup>1</sup>, Harrilla Profka<sup>1</sup>, Jennia Rajaei<sup>1</sup>, Stephen J. Kadlecck<sup>1</sup>, Masaru Ishii<sup>2</sup>, and Rahim R. Rizi<sup>1</sup>

<sup>1</sup>Radiology, University of Pennsylvania, Philadelphia, PA, United States, <sup>2</sup>Otolaryngology - Head and Neck Surgery, Johns Hopkins University, Baltimore, MD, United States

**INTRODUCTION:** Pulmonary ventilation is a key marker in obstructive lung diseases, and its non-invasive imaging can provide insight into severity and distribution of obstructive lung diseases. Respiratory gas arrival and distribution time parameters can substantially vary within the lung and among different subjects, and can be a suitable metric to quantify the alterations in airway resistance and obstruction. These parameters can be potentially measured on a regional basis and at a high resolution using hyperpolarized (HP) gas MRI technology. In this work we present a technique for regional measurement of temporal distribution of respiratory gas in the lungs of mechanically ventilated animals.

**METHODS:** Previous work has used a lumped three-compartment respiratory model to image *steady state* fractional ventilation in mechanically ventilated animals [1]. Yet in such a model, it was assumed that the arriving gas content from the conductive airways, with magnetization  $M_C$ , had completely and uniformly mixed with the residual gas content in acinar airways, leading to the resulting magnetization  $M_A$ , before images were acquired. This assumption is fairly reasonable if a long enough pre-acquisition time delay (PAD) is incorporated in the ventilation imaging pattern as shown in **Figure 1**. The choice of the PAD, however, can have a significant impact on the measured  $r$  value. A too short time delay can potentially underestimate  $r$ , due to inadequate arrival and mixing of respiratory gas. A longer time delay provides a cushion against this effect, but promotes a more substantial signal decay in the presence of oxygen, and also deviates the ventilatory pattern further away from the normal respiratory rate. The uniform mixing assumption may also be affected by the presence of obstructive lung diseases with elevated airway resistance. In order to assess the transitional effect of respiratory gas arrival and mixing on fractional ventilation measurements,  $r$  can in general be defined as a function of time over the timescale of each breath. The magnetization build-up can then be described as:

$$M_A(j, t) = r(t) \cdot M_T(j-1, t) + [1-r(t)] \cdot M_A(j-1, t) \cdot \exp\left[-N_{PE} \ln(\cos \alpha) - t \cdot pO_2 / \xi\right] \quad [1]$$

where  $r(t) = r_f [1 - \exp(-t/T_r)]$  ( $r(0) = 0$ ) represents the progressively increasing fraction of fresh gas arriving in

the airways with each breath, where  $N_{PE}$ : number of RF pulses (phase encoding lines),  $\alpha$ : flip angle,  $pO_2$ : partial pressure of oxygen, and  $\xi = 2.6$  mbar-sec. The fraction of fresh gas approaches the steady state (final) value  $r_f$  with the time constant of  $T_r$ . When the pre-acquisition delay is larger or of the same order of magnitude of  $T_r$ , the assumption of constant fractional ventilation holds:  $r = \lim_{T_r \ll PAD} r(t) = r_f$ .

In order to assess the regional distribution of the fractional ventilation time constant  $T_r$ ,  $r$  measurements were performed in the similar fashion described in [1] in rat lungs, with the only difference that PAD was varied in 12 unequal steps from 0 to 3 seconds, according to: PAD = 0, 100, 200, 250, 300, 350, 400, 500, 750, 1000, 2000 and 3000 msec. Measurements were performed in two rats (440 g body weight,  $V_T = 10$  mL/kg), and repeated three times in each animal with staggered ordering in order to distribute the effect of external relaxation of HP gas across multiple measurements. The  $r$  maps from different time points were co-registered using a standard affine transformation by using the  $r$  map corresponding to PAD=3000 sec as the reference image. This step was performed in order to correct for any spatial mismatch caused by different inflation level corresponding to varying respiratory time points. The breathing gas was switched to <sup>3</sup>He:O<sub>2</sub>=4:1 over ten breaths for ventilation imaging. A gradient echo MRI pulse sequence was used on the middle coronal slice with FOV=5×5cm<sup>2</sup> (64×64 matrix size), ST=5mm, TR/TE=4.8/3.3ms, and  $\alpha \approx 5^\circ$ .

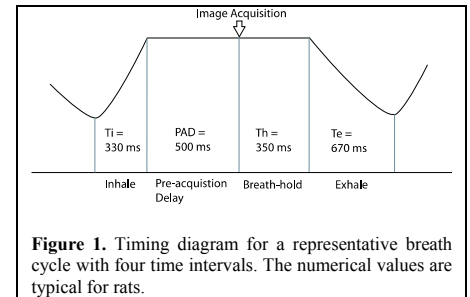


**Figure 1.** Timing diagram for a representative breath cycle with four time intervals. The numerical values are typical for rats.

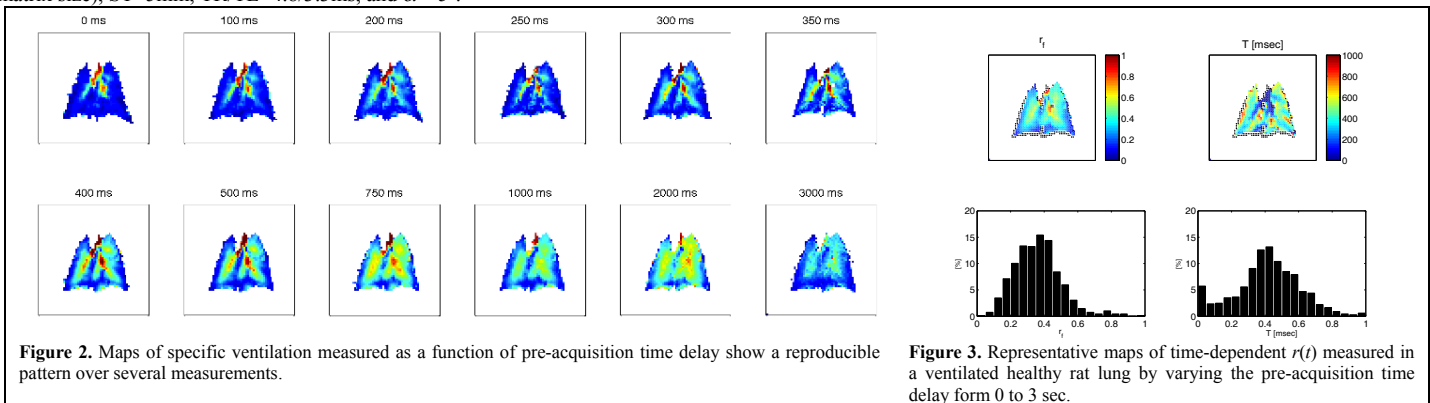


**Figure 2.** Maps of specific ventilation measured as a function of pre-acquisition time delay show a reproducible pattern over several measurements.

**Figure 3.** Representative maps of time-dependent  $r(t)$  measured in a ventilated healthy rat lung by varying the pre-acquisition time delay from 0 to 3 sec.

**RESULTS:** Averaged maps of  $r(t)$  computed as a function of pre-acquisition time delay are shown in **Figure 2** for a representative study. The variable time delay allows for capturing *almost* instantaneous states of respiratory gas distribution in the airways. This in turn allowed us to explicitly solve for the gas arrival time constant and delay on a regional basis. A representative resulting map of  $r_f$  (steady state  $r$ ) and the corresponding ventilation time constant are shown in **Figure 3** for one rat.  $r_f = 0.26 \pm 0.13$ ,  $T_r = 352 \pm 166$  msec in the first rat, and  $r_f = 0.36 \pm 0.14$ ,  $T_r = 416 \pm 191$  msec in the second rat. The black dots on these two diagrams represent the voxels that were enclosed in the lung but did not fit properly to the fractional ventilation time constant model, **Equation 1**. Voxels enclosed within conductive airways (including trachea and major bronchi) almost unanimously exhibit a near zero time constant which supports the relatively immediate gas transport process in these major airways. In contrast the majority of the voxels enclosed within the lung parenchyma show a time constant around  $T_r=400$  msec, which is smaller than the PAD=500 msec time delay used in small animal results reported earlier.

**DISCUSSION AND CONCLUSION:** Introduction of controlled pre-acquisition time delay in the existing specific ventilation imaging technique provides a tool for determining the regional gas arrival time constant, with a fairly similar implication to lung RC time constants on a regional basis. Co-registration of images and possible lung motion during the actual image acquisition (300ms approx.), especially for very short time pre-acquisition time delays, can be a source of error in matching images from different time points. This effect is mostly evident at the points near the diaphragm and on the edges where the fit was ill-posed (shown as black dots). Performing the imaging at end-expiration versus end-inspiration can largely address this issue, although at a price of a worse signal-to-noise ratio. Results can alternatively be utilized to select a proper pre-acquisition time delay to minimize motion-induced errors and well mixing of inspired and residual gases in standard specific ventilation imaging applications with HP gas MRI. The ventilation time constant has the potential to be used to quantify obstructive lung disease or any lung disease that in any way affects ventilation or ventilation efficiency on a regional basis. Evaluation of this metric in obstructive lung disease models presents a natural next step to affirm its utility.

**REFERENCES:** [1] Emami K, *et al.*, Magn Reson Med. 2010 Jan; 63(1):137-50.